Computational Modeling Study on Formation of Acyclic Clavulanate Intermediates in Inhibition of Class A β-Lactamase: Water-Assisted Proton Transfer

Rui Li, Dacheng Feng,* and Shengyu Feng

Shandong University, School of Chemistry and Chemical Engineering

Received: October 30, 2008; Revised Manuscript Received: December 12, 2008

Molecular dynamics (MD) simulation and quantum chemical (QC) calculations were used to investigate the reaction mechanism of the formation of acyclic clavulanate intermediates in the inhibition of class A β-lactamase. The initial model for QC calculations was derived from an MD simulation. It was composed of a substrate clavulanate and four residues (Ser70, Gln237, Ser130, and Ser216), which form hydrogen bonds with the substrate. The QC calculation results indicate that the oxazolidine ring can undergo cleavage by proton transfer, which yields not only imine but also enamine products. A new mechanism involving hydrogen transfer from C6 to O1 has been suggested. Besides, MD simulation provided evidence that the water molecule can catalyze the proton transfer, and QC calculation shows water assistance can decrease the energy barrier greatly.

1. Introduction

β-lactam antibiotics are clinically important drugs, which are used as effective agents against bacterial diseases on account of their effectiveness and low toxicity.[1] However, the appearance of β-lactamases presents a serious and growing threat to the efficacy of antibacterial chemotherapy and thus it becomes a major challenge to human health.[2] On the basis of the activity site differences, these β-lactamases have been divided into four classes, A−D.[3] Those of class B β-lactamases are metalloenzymes, whereas classes A, C, and D are serine enzymes. One strategy for overwhelming β-lactamase-mediated resistance is the coadministration of a β-lactam antibiotic and a β-lactamase inhibitor. β-lactamase inhibitor can bind to β-lactamases to make them inactive, consequently protecting the antibiotics.[4]

Clavulanic acid, an inhibitor for class A β-lactamases, was the very first inhibitor for an antibiotic resistance enzyme that found clinical utility in 1985.[5] The process of inhibition of the class A β-lactamases by the Clavulanate is complicated, and there have been some experimental studies on it.[6−9] A common mechanism (Figure 1) has been proposed: the Ser70-OH of β-lactamases attacks the carbon (C7) of the carbonyl group in the β-lactam ring. This leads to the acyl−enzyme intermediate (AEI). AEI undergoes further reaction to generate a linear imine species after oxazolidine ring opening and departure of the oxygen from C5. This imine proceeds next to cis and trans enamine via rearrangement.

Chen and Herzberg determined the crystal structure of β-lactamase from *Staphylococcus aureus* PC1 by a 2.2 Å resolution cryocrystallographic study.[6] They trapped enzyme−clavulanate complex, which formed the Ser-70-attached *cis*-enamine as well as *trans*-enamine. However, the mechanism of oxazolidine ring opening is still unclear. Lin et al. modeled the alkaline hydrolyses of Clavulanate using an ab initio quantum method.[10] In their studies, N4 hydrogen was transferred to O1 to yield an imine product, which in turn can isomerize to form a less-stable enamine product. In the present article, we investigated the mechanism of formation of acyclic clavulanate intermediates in inhibition of class A β-lactamase using MD and OC methods. Herein, a new mechanism was suggested: the enamine product can be directly obtained via hydrogen transfer from C6 to O1. To compare, we also study the common mechanism viz. hydrogen transfer from N4 to O1, which yields an imine product.

* To whom correspondence should be addressed. E-mail: fdc@sdu.edu.cn. Tel: +86-531-88365748. Fax: +86-531-88564464.

2. Models and Methods

2.1. Construction of the Initial Model. First, we need the structure of the AEI as the initial model for quantum chemical calculation. The data on the 3D structure of the class A β-lactamase from *S. aureus* PC-1 and clavulanate moiety have been deposited in the Protein Data Bank (1BLC),[6] and we constructed the initial model from it. In the original PDB data, both the β-lactam ring and the adjacent oxazolidine ring had been cleaved. So, we rebuilt the AEI by closing the oxazolidine ring in 1BLC. To get the reasonable structure, energy minimization and MD calculation were performed. These computations were carried out by means of the *Gromacs 3.2* program.[11] The gromacs force field was applied, and the force field parameter of substrate was generated by the PRODRG server.[12] The solvent used was the SPC water model,[13] and the periodic box size was 65.2 Å × 42.1 Å × 52.1 Å. The chloride ions as counterions were added to neutralize the net charge. For long-range electrostatics, the particle mesh Ewald (PME)[14] method was applied. The Coulomb term and van der Waals interaction were truncated at 9 Å. The LINCS[15] algorithm was employed to satisfy the bond constraints.

First of all, the energy minimization was performed. In the energy minimization on the system, the steepest descent method was performed in early cycles and then the conjugate gradient method was performed latter. Then we ran a position-restrained dynamics simulation, which restrained the atom positions of the macromolecule while letting the solvent move in the simulation, and this used 20 ps. The simulation was performed at constant temperature and pressure by coupling the system to a Berendsen bath[16] at 300 K and at 1 atm. Finally, a 1 ns MD trajectory is performed for the system. Root-mean-square deviation (rmsd) time series (Figure 2) suggest that the system was well equilibrated after about 500 ps.

10.1021/jp809605t CCC: $40.75
Published on Web 02/03/2009

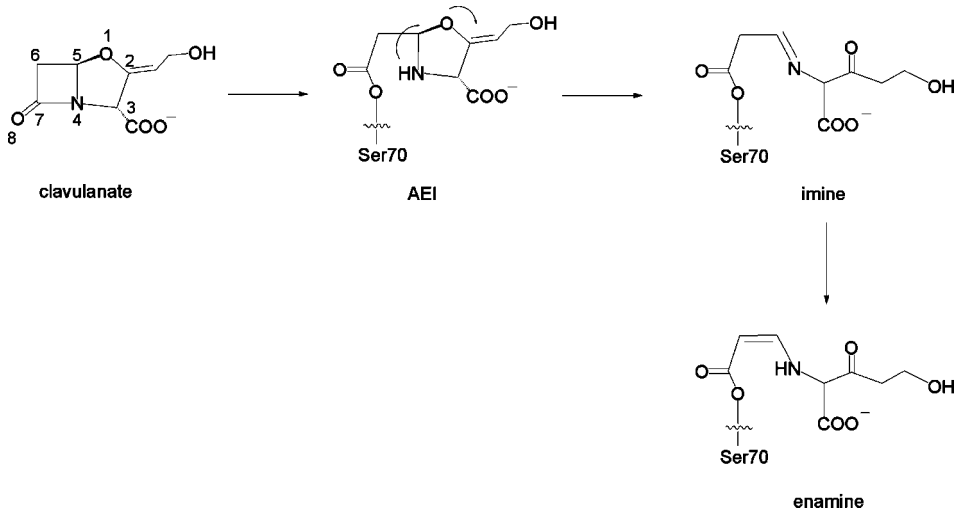

Figure 1. Common mechanism for clavulanate inhibition of class A β-lactamase.

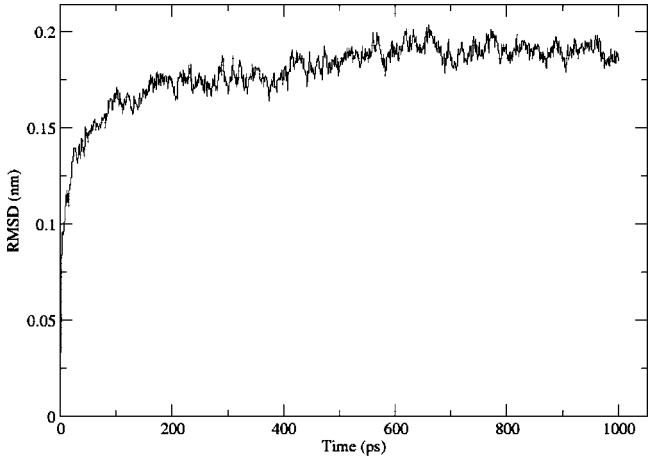

Figure 2. Root-mean-square deviation (rmsd) of the AEI structure during MD simulation.

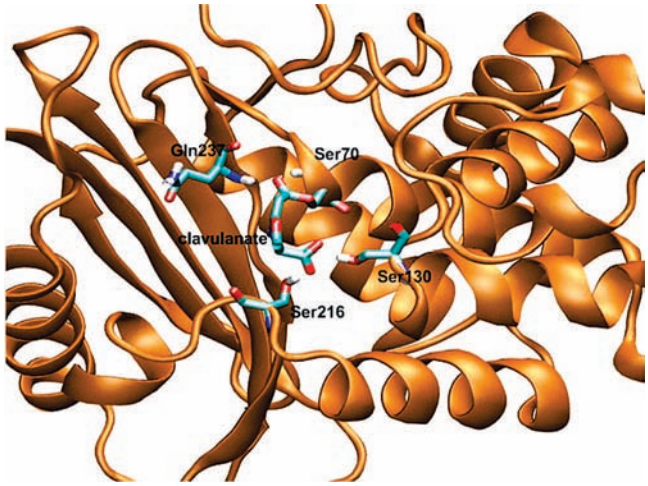

Figure 3. Substrate clavulanate as well as residues in the active site.

The average structure between 500 and 1000 ps in MD calculation was obtained via the g_rmsf tool in the *Gromacs* package. The active stie structure is shown in Figure 3. It has been found that four amino acid residues are located around the degraded substrate and contribute to the stability of the substrate (Ser70, Ser130, Ser 216, and Gln237). They were extracted for the next QC calculation.

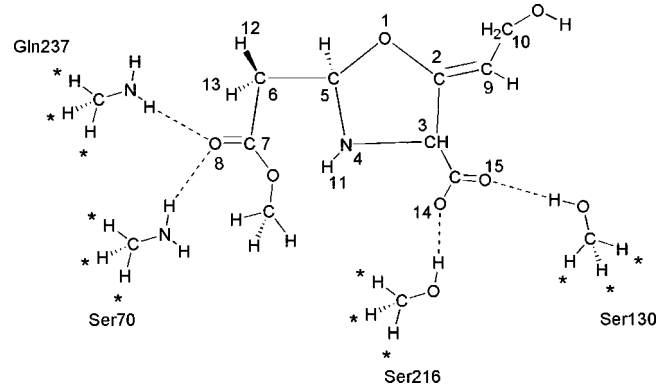

Figure 4. Initial model for quantum chemistry calculations.

2.2. Quantum Chemical Calculation. To study the detailed mechanism, quantum chemical calculation is necessary. The structure of the QC model is shown in Figure 4. The truncated residues were replaced with hydrogen atoms and they were fixed in the QC calculations. The B3LYP set of the density functional theory (DFT)[17,18] method, which is very well-suited for model enzyme active sites and reaction mechanisms was used.[19] The geometries of reactants, intermediates, transition states, and products were fully optimized at the 6-31G* level. All energies were calculated including zero-point vibrational energy (ZPE). Solvent effects were taken into consideration implicitly, through single point calculations on the optimized geometries at the same level of theory, including the polarized continuum model (PCM),[20] and the radii type for the PCM calculation is UAHF. Water was used as solvent, through the value 78.39 for the dielectric constant in the PCM calculations. To establish the connection between the transition structures and corresponding equilibrium structures, the reaction pathways were followed using the intrinsic reaction coordinate (IRC)[21] procedure. These calculations have been carried out using the *Gaussian 03*[22] package of programs.

3. Results and Discussion

3.1. Active Site Structure. In the active site structure of the AEI (Figure 3), Ser 70 and Gln237 are around the oxygen of the β-lactam carbonyl group (O8). The average distances of O8-HN@Ser70 and O8-HN@Gln237 were 1.86 Å and 1.74 Å respectively during the MD simulation. It indicated that two hydrogen bonds were formed. This interaction reflects the role

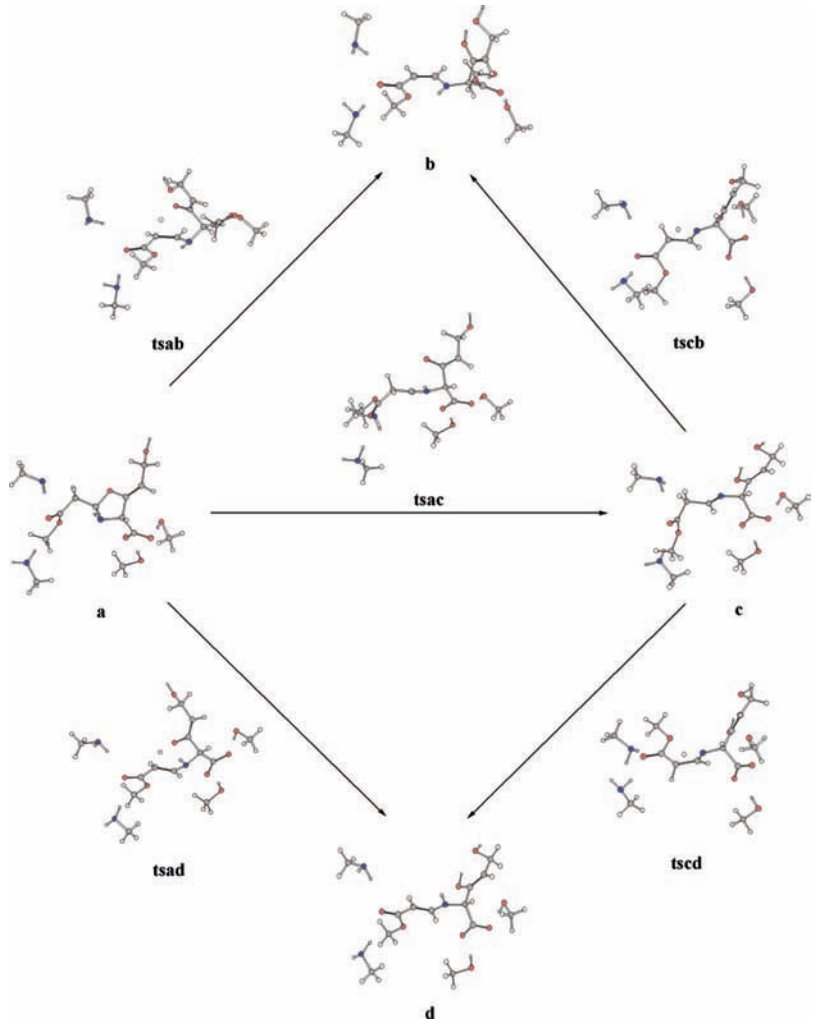

Figure 5. Overall reaction paths.

of the oxyanion hole that consists of two NH groups of the main chains in Ser70 and Gln237.[23] In previous molecular dynamics simulations of the class A β-lactamase complexed with other β-lactam compounds (penicillin, cephalothin),[24−26] the effect of the oxyanion hole has been mentioned. In these studies, the β-lactam ring was closed and the oxyanion hole was well around the closed β-lactam ring to stabilize the O8. In the present study, the β-lactam ring was completely cleaved. However, the oxyanion hole was still preserved. It suggests the oxyanion hole plays an important role in the mechanism of clavulanate-inhibiting class A β-lactamase.

Besides, the oxygen atoms of the C3-carboxyl group (O14 and O15) interacted with the hydroxyl group of the Ser216 and Ser130, respectively. The average distances of O14- HO@Ser216 and O15-HO@Ser130 were 1.71 Å and 1.68 Å, repectively. Ser130 also is an important residue. It has been reported that not only does Ser130 take part in the substrate binding but also it assists the substrate acylation and deacylation.[27,28]

3.2. Oxazolidine Ring Opening. Figures 5 and 6 show the overall mechanisms that were carefully studied by us as well as the optimized reactants, transition states, and products structures. Energies of all of the stationary points are summarized in Tables 1 and 2.

The initial structure **a** was optimized. In the structure of **a**, the lactam ring was opened, whereas oxazolidine ring was closed. There are two hydrogens on the C6 (H12 and H13). H12 locates above the C5−C6−C7 plane, whereas H13 locates below the plane (Figure 4). Both hydrogens are close to O1, and distances are 2.66 Å and 2.63 Å, respectively. So, the hydrogen migration from C6 to O1 will be a reasonable assumption even though there's no such reaction referred in the well-known mechanism. This assumption is supported by our calculations.

H12 is away from C6 and attack to O1 then brings on the cleavage of the oxazolidine ring. The transition-state structure of this process is **tsab**, and the energy barrier is 39.00 kcal/mol. For **tsab**, the distances of C6−H12, O1−H12, and O1−C5 are 1.32, 1.42, and 2.33 Å, respectively. Following the leaving of H12, the hybridization of C6 becomes sp^2 from the original sp^3. The dihedral N4−C5−C6−C7 becomes −27.5° compared to −61.7° in **a**. An IRC calculation on **tsab** led to reactant **a** on the one hand and to product **b** on the other. The relative energy of **b** is −1.80 kcal/mol. For structure **b**, the O1−C5 distance is 2.99 Å, and the O1−H12 bond distance is 0.98 Å. It is obvious that the oxazolidine ring is completely opened and H12 has been transferred to O1. **b** is a *cis*-enamine form structure. In **b**, the dihedral N4−C5−C6−C7 is 2.5°, and the bond length C5−C6 is 1.38 Å.

Similarly, H13 can also attack to O1. However, it follows a different path owing to an opposite geometric location. The transition state of this process is **tsad**. In **tsad**, the dihedral N4−C5−C6−C7 is −164.2° compared −27.5° in **tsab**. This process is subject to an activation energy of 39.09 kcal/mol compared to 39.00 kcal/mol in **tsab**. It reveals that the energy

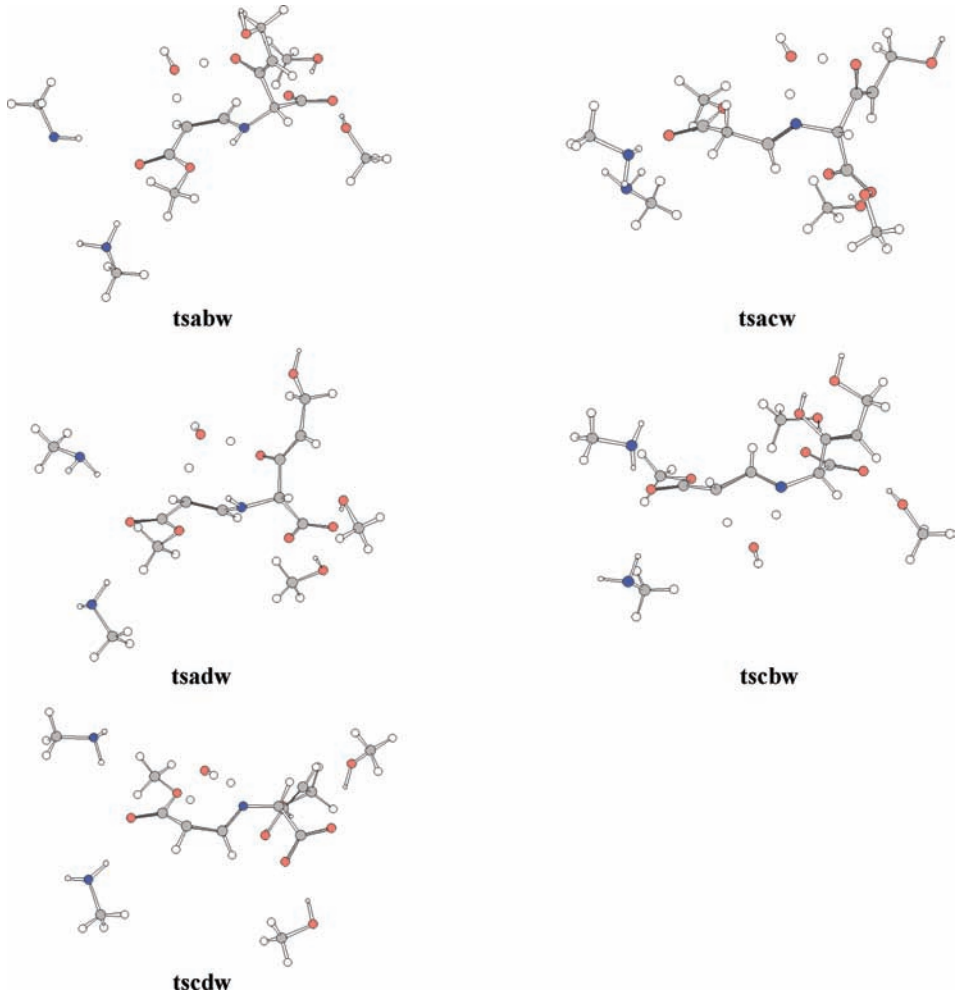

Figure 6. Transition states in the water-assisted mechanism.

TABLE 1: Energies of all Structures in Non-Water-Assisted Mechanism[a]

	E + ZPE	rel. energy	E + ZPE (PCM)	rel. energy (PCM)
a	−1279.02317	0	−1279.13651	0
tsab	−1278.96101	39.00	−1279.06587	44.32
b	−1279.02604	−1.80	−1279.13009	4.03
tsad	−1278.96088	39.09	−1279.07193	40.52
d	−1279.02643	−2.04	−1279.13202	2.81
tsac	−1278.95947	39.97	−1279.06871	42.55
c	−1279.00684	10.25	−1279.11482	13.61
tscb	−1278.93867	53.03	−1279.04399	58.06
tscd	−1278.94248	50.63	−1279.04401	58.04

[a] E and ZPE in hartree and relative energies in kcal/mol.

barrier is not affected by the reverse conformation change. The product of this process is **d**. The relative energy of **d** is −2.04 kcal/mol. In structure **d**, the dihedral N4−C5−C6−C7 is −175.8°, the bond length of C5−C6 is 1.37 Å, and it is a *trans*-enamine form structure.

To compare, we also simulated the common path for oxazolidine ring opening, viz. the H11 transfer from N4 to O1. The transition state of this process is **tsac**. The energy barrier of this process is 39.97 kcal/mol and an imine product **c** is obtained. In structure **c**, the dihedral C3−N4−C5−C6 is −177.0° and the bond length of N4−C5 is 1.27 Å. The relative energy of **c** is 10.25 kcal/mol, which is higher than that of enamine products.

For all of the three oxazolidine ring opening paths, activation energies obtained are so large that the reactions cannot proceed practically. Moreover, the solvent effect cannot decrease the energy barrier (Table 1). However, direct hydrogen transfer might be assisted by some water molecule bridge. The evidence has been found: in the MD simulation, the shortest distances between water molecules and O1, water molecules and N4, and water molecules and C6 are about 0.24, 0.26, and 0.23 nm, respectively (Figure 7). These distances are appropriate for water assistance; viz. a water molecule can act as a bridge-connecting H-donor and H-acceptor. For paths **a**−**b**, **a**−**c**, and **a**−**d**, the water-assisted transition states are **tsabw**, **tsacw**, and **tsadw**, respectively (Figure 6).

To calculate the energy barrier of water-assisted process, it is required to get the energy of reactants and products in each reaction step combined with water. Because we adopt a simple model, directly optimization on these hydrates will arise unsuitability changes of the model (however, in the transition state, there is no problem because the water molecular is a bridge of the H migration, which is fixed between two groups). Therefore, we define that the energies of these hydrates are

$$E_{XW} = E_X + E_W - E_H$$

In the formula, E_X are the energies of anhydrous compound, E_W is the energy of one water molecule (−76.38779 au at the B3LYP/6-31G* level), and E_H is the hydrogen bond energy, which combine a water molecule. Here, E_H is different according the atom, which links hydrogen bond. In our article, the atoms

TABLE 2: Energies of all Structures in Water-Assisted Mechanism[a]

	E + ZPE	E_{XW}	rel. energy	E + ZPE (PCM)	E_{XW} (PCM)	rel. energy (PCM)
aw1		−1355.41268	0		−1355.52602	0
tsabw	−1355.38864		15.08	−1355.49616		18.73
tsadw	−1355.38805		15.45	−1355.50018		16.21
aw2		−1355.41529	−1.63		−1355.52863	−1.63
tsacw	−1355.38680		16.23	−1355.50319		15.96
cw		−1355.39635	10.25		−1355.50433	13.61
tscbw	−1355.38051		20.18	−1355.48579		25.24
tscdw	−1355.38218		19.14	−1355.48584		25.21

[a] E and ZPE in hartree and relative energies in kcal/mol.

N4 and C6 are involved, so we evaluate the hydrogen bond energy of $(CH_3)_2NH-OH_2$ (0.00433 au) and $(CH_3)_2CH_2-OH_2$ (0.00172 au) to be E_H approximatively, respectively. In paths **a**−**b** and **a**−**d**, C6 is linked to a hydrogen bond, so the hydrate energy (Eaw1) is −1355.412681 au. In path **a**−**c**, N4 is linked to a hydrogen bond, so the hydrate energy (Eaw2) is −1355.415291 au. In our earlier work, this method has been used on the study of the 6-methylidene penem inhibition mechanism.[29] This method does not consider the interaction between the water molecule and the reactant sufficiently, so the results show that the monohydration hardly affects the monohydrate's relative stability. However, the error should be small and cannot affect the reaction paths.

Energies of all of the stationary points in the water-assisted process are summarized in Table 2. The energy barriers of paths **a**−**b**, **a**−**d**, and **a**−**c** are 15.08, 15.45, and 16.23kcal/mol, respectively. It is obvious that the energy barriers are decreased greatly.

3.3. Imine−Enamine Tautomerization. The common mechanism has suggested the imine form can be rearranged to the enamine form, and our calculations also follow this. The relative energy of imine **c** is higher than those of enamine products, so

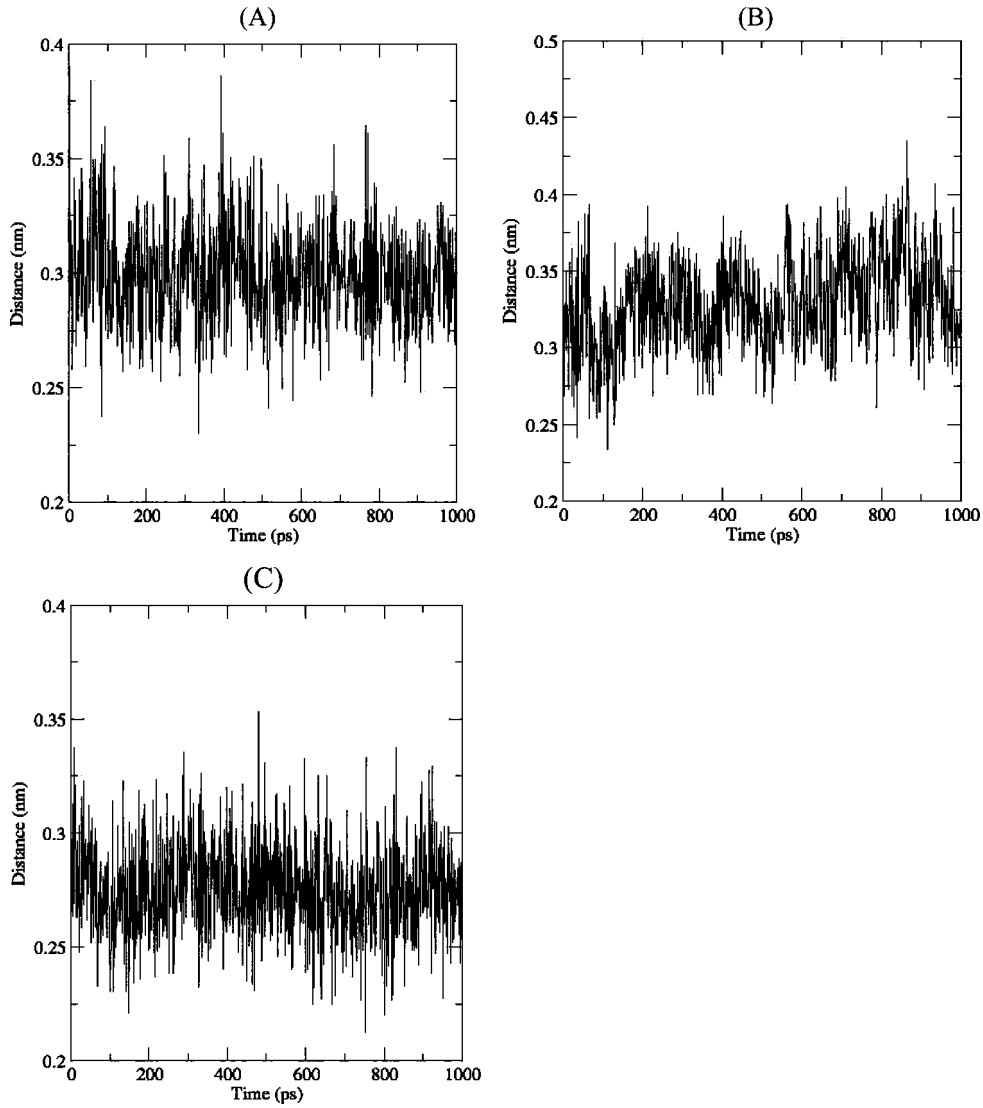

Figure 7. Variation of the minimum distance between the water molecule and (A) O1, (B) N4, and (C) C6 during MD simulation. They were obtained via the g_mindist tool in the *Gromacs* package.

these rearrangement reactions are thermodynamics-favored. We considered that the imine−enamine tautomerism involves hydrogen transfer from C6 to N4.

In imine **c**, H12 locates below the N4−C5−C6 plane, whereas H13 locates above the plane (Figure 6). They are close to N4, and the distances are 2.58 Å and 2.88 Å, respectively. Both H12 and H13 can be transferred to N4 from C6. However, the different products can be obtained as a result of different transfer paths. The H12 transfer yields *cis*-enamine **b** through a transition-state **tscb**, and the activation energy is 42.78 kcal/mol. In **tscb**, the dihedral angle O1−C2−C9−C10 is −128.5° compared to −155.0° in **c**. It is obvious that C5−C6 undergoes a rotation lead to the formation of a *cis*-enamine conformation. The H13 is transferred to N4 through transition-state **tscd** to yield *trans*-enamine **d**, and the activation energy is 40.38 kcal/mol. In **tscd**, the dihedral angle O1−C2−C9−C10 is 113.3°, which indicates a C5−C6 rotational orientation different from the one in **tscb**.

Similarly, the imine−enamine tautomerization also can be assisted by a water molecule, and the transition states are **tscbw** and **tscdw** (Figure 6), respectively. The energy barriers of paths **c**−**b** and **c**−**d** are 9.93 and 8.89 kcal/mol, respectively.

4. Conclusions

We have studied the reaction mechanism for clavulanate-inhibiting β-lactamase. The initial AEI model was derived from MD simulation. The four residues Ser70, Gln237, Ser130, and Ser216 which form hydrogen bonds with the substrate were considered in quantum chemistry calculation. In all of the reaction paths, these hydrogen bonds are retained.

The mechanism includes the opening of the oxazolidine ring and enamine−imine tautomerization. The oxazolidine ring undergoes cleavage as a result of hydrogen transfer from C6 or N4 to O1, and three different products (*cis*-enamine, *trans*-enamine, and imine) are obtained. The active energies of the three reaction paths are very close.The new mechanism is that the enamine product can be directly obtained via hydrogen transfer from C6 to O1. Comparing the three acyclic products, the imine form **c** is the most unstable conformation, which is rearranged to the enamine form **b** and **d** via hydrogen transfer from C6 to N4. It is concluded that the complexity of reactions enhances the inhibition ability of clavulanate.

The activation energies of all of the reactions are very large. However, these reactions can be assisted by a water molecule, which is supported by our MD simulation. Compared with the solvent effect, water assistance affects the active energy greatly. Water assistance can shorten the distance of hydrogen migration. Moreover, it would hardly distort the well-balanced structure and has a relaxed transition state in each process. So, water assistance significantly decreases the activation energies, and thus the reactions can proceed practically.

Acknowledgment. The Research work was supported by the National Natural Science Foundation of China (No. 20574043) and Natural Science Foundation of Shandong Province (Z2007B02).

Supporting Information Available: The Cartesian coordinates of all stationary points under study. This material is available free of charge via the Internet at http://pubs.acs.org.

References and Notes

(1) Frère, J.-M.; Joris, B. *Crit. Rev. Microbiol.* **1985**, *11*, 299.
(2) Davies, J. *Science* **1994**, *264*, 375.
(3) Ambler, R. P. *Philos. Trans. R. Soc. London, Ser. B* **1980**, *289*, 321.
(4) Page, M. I.; Laws, A. P. *Chem. Commun.* **1998**, 1609.
(5) Lee, N.; Yuen, K. Y.; Kumana, C. R. *Drugs* **2003**, *63*, 1511.
(6) Chen, C. C.; Herzberg, O. *J. Mol. Biol.* **1992**, *224*, 1103.
(7) Brown, R. P. A.; Aplin, R. T.; Schofield, C. J. *Biochemistry* **1996**, *35*, 12421.
(8) Swarén, P.; Golemi, D.; Cabantous, S.; Bulychev, A.; Maveyraud, L.; Mobashery, S.; Samama, J.-P. *Biochemistry* **1999**, *38*, 9570.
(9) Sulton, D.; Pagan-Rodriguez, D.; Zhou, X.; Liu, Y.; Hujer, A. M.; Bethel, C. R.; Helfand, M. S.; Thomson, J. M.; Anderson, V. E.; Buynak, J. D.; Ng, L. M.; Bonomo, R. A. *J. Biol. Chem.* **2005**, *280*, 35528–35536.
(10) Lin, Y.-l.; Chang, N.-y.; Lim, C. *J. Am. Chem. Soc.* **2002**, *124*, 12042.
(11) Lindahl, E.; Hess, B.; Spoel, D. v. d. *J. Mol. Mod.* **2001**, *7*, 306–317.
(12) Schuettelkopf, A. W.; Aalten, D. M. F. v. *Acta Crystallogr.* **2004**, 1355.
(13) Berendsen, H. J. C.; Postma, J. P. M.; van Gunsteren, W. F.; Hermans, J. Interaction Models for Water in Relation to Protein Hydration. In: *Intermolecular Forces*; Pullman, B., Ed.; D. Reidel Publishing Company: Dordrecht, The Netherlands, 1981; 331.
(14) Darden, T. A.; York, D. M.; Pedersen, L. G. *J. Chem. Phys.* **1993**, *98*, 10089.
(15) Hess, B.; Bekker, H.; Berendsen, H. J. C.; Fraaije, J. G. E. M. *J. Comput. Chem.* **1997**, *18*, 1463.
(16) Berendsen, H. J. C.; Potsma, J. P. M.; van Gunsteren, W. F.; DiNola, A. D.; Haak, J. R. *J. Chem. Phys.* **1984**, *81*, 3684.
(17) (a) Becke, A. D. *J. Chem. Phys.* **1993**, *98*, 5648−5652. (b) Lee, C.; Yang, W.; Parr, R. G. *Phys. Rev. B* **1988**, *37*, 785–789. (c) Stephens, P. J.; Devlin, F. J.; Chabalowski, C. F.; Frisch, M. J. *J. Phys. Chem.* **1994**, *98*, 11623–11627.
(18) Lee, C.; Yang, W.; Parr, R. G. *Phys. Rev. B* **1988**, *37*, 785.
(19) Himo, F. *Theor. Chem. Acc.* **2006**, *116*, 232–240.
(20) Tomasi, J.; Persico, M. *Chem. Rev.* **1994**, *94*, 2027.
(21) Gonzalez, C.; Schlegel, B. *J. Phys. Chem.* **1990**, *94*, 5523.
(22) Frisch, M. J. T., G. W.; Schlegel, H. B.; Scuseria, G. E.; Robb, M. A. C., J. R.; Montgomery, J. A., Jr.; Vreven, T.K., K. N.; Burant, J. C.; Millam, J. M.; Iyengar; S. S.; Tomasi, J. B., V.; Mennucci, B.; Cossi, M.; Scalmani; G.; Rega, N. P., G. A.; Nakatsuji, H.; Hada, M.; Ehara, M. T., K.; Fukuda, R.; Hasegawa, J.; Ishida, M.; Nakajima, T. H., Y.; Kitao, O.; Nakai, H.; Klene, M.; Li; X.; Knox, J. E. H., H. P.; Cross, J. B.; Bakken, V.; Adamo, C. J., J.; Gomperts, R.; Stratmann, R. E.; Yazyev, O. A., A. J.; Cammi, R.; Pomelli, C.; Ochterski, J. W.; Ayala, P. Y. M., K.; Voth, G. A.; Salvador, P.; Dannenberg, J. J. Z., V. G.; Dapprich, S.; Daniels, A. D.; Strain, M. C. F., O.; Malick, D. K.; Rabuck, A. D.; Raghavachari, K. F., J. B.; Ortiz, J. V.; Cui, Q.; Baboul, A. G. C., S.; Cioslowski, J.; Stefanov, B. B.; Liu, G.; Liashenko, A. P., P.; Komaromi, I.; Martin, R. L.; Fox, D. J. K., T.; Al-Laham, M. A.; Peng, C. Y.; Nanayakkara, A.; Challacombe, M. G., P. M. W.; Johnson, B.; Chen, W. W., M. W.; Gonzalez, C.; Pople, J. A. *Gaussian 03*;CT, 2004.
(23) Herzberg, O. *J. Mol. Biol.* **1991**, *217*, 701.
(24) Díaz, N.; Sordo, T. L.; Jr, K. M. M.; Suárez, D. *J. Am. Chem. Soc.* **2003**, *125*, 672.
(25) Díaz, N.; Suárez, D.; Kenneth M. Merz, J.; Sordo, T. L. *J. Med. Chem.* **2005**, *48*, 780.
(26) Fujii, Y.; Okimoto, N.; Hata, M.; Narumi, T.; Yasuoka, K.; Susukita, R.; Suenaga, A.; Futatsugi, N.; Koishi, T.; Furusawa, H.; Kawai, A.; Ebisuzaki, T.; Neya, S.; Hoshino, T. *J. Phys. Chem.* **2003**, *107*, 10274.
(27) Díaz, N.; Suárez, D.; Sordo, T. L.; Kenneth M. Merz, J. *J. Phys. Chem. B* **2001**, *105*, 11302.
(28) Fujii, Y.; Hata, M.; Hoshino, T.; Tsuda, M. *J. Phys. Chem. B* **2002**, *106*, 9687.
(29) Li, R.; Feng, D.; He, M. *J. Phys. Chem. A* **2007**, *111*, 4720.

JP809605T